

# Linear Optical Implementation of a Quantum Network for Quantum Estimation

Zhi-Wei Wang, Jian Li,\* Yun-Feng Huang,<sup>†</sup> Yong-Sheng Zhang, Xi-Feng Ren, Pei Zhang, and Guang-Can Guo<sup>‡</sup>

*Key Laboratory of Quantum Information,  
University of Science and Technology of China,  
CAS, Hefei 230026, People's Republic of China*

## Abstract

We present a scheme for simulating the quantum network of quantum estimation proposed by A. K. Ekert *et al.* [Phys. Rev. Lett. 88, 217901 (2002)]. We experimentally implement the scheme with linear optical elements. We perform overlap measurements of two single-qubit states and entanglement-witness measurements of some two-qubit states. In addition, it can also be used for entanglement quantification for some kinds of states. From the other perspective, we physically realize the positive but not completely positive map, transposition.

PACS number(s): 03.67.Lx, 42.50.Dv, 03.67.-a

---

\*Electronic address: jianli@ustc.edu.cn

<sup>†</sup>Electronic address: hyf@ustc.edu.cn

<sup>‡</sup>Electronic address: gctuo@ustc.edu.cn

A density matrix can completely characterize the state of a quantum system. For low dimensional systems, quantum estimations of density matrices are well mastered. Then the properties of the quantum state, which can be quantified in terms of linear or nonlinear functionals of density matrices, can be extracted from it. However, for high dimensional systems, the state reconstruction becomes very difficult and a direct estimation of a specific quantity may be more efficient. Thus one quantum network (shown in Fig. 1) and its related idea are presented in [1, 2, 3, 4], which can be used as a basic building block for direct quantum estimations of both linear and nonlinear functionals of any density operator. The network can perform overlap measurements of two single-qubit states and entanglement-witnessmeasurements [5] of some two-qubit states. In addition, it can also be used for entanglement quantification for some kinds of states.

In this paper, we put forward a scheme to simulate the network and experimentally realize it using linear optical elements. In Fig. 1, the network is a one-qubit interferometric setup (consisting of two Hadamard gates and phase shift, followed by a measurement in the computational basis) modified by inserting a controlled-SWAP operation between the two Hadamard gates, with its control on the single qubit and SWAP on an unknown system described by density operator  $\rho_a \otimes \rho_b$ . Our scheme is based on two Hong-Ou-Mandel interferometers [6]. The scheme set-up is shown in Fig. 2 (a). A  $\beta$ -barium borate (BBO) crystal arranged in the Kwiat type configuration [7] is pumped by a UV laser beam. Through the spontaneous parametric down-conversion (SPDC) process, an entangled state of the form

$$a|HH\rangle + b|VV\rangle \quad (1)$$

is produced, where  $H$  and  $V$  represent horizontal and vertical polarization of photons respectively. By means of this entanglement source, some simple optical elements and optical set-ups, such as half wave plate (HWP), quarter wave plate (QWP) and quartz, we can prepare some other kinds of entangled states and mixed states [8]. Then we can put the prepared states into the quantum network. The path of the two-photon is selected as the control qubit while the target qubits have many choices, such as polarization, spatial mode, moment and other freedom degrees of the photon. For simplicity, here we just encode the qubit with polarization of the photon.

In general, we suppose that after state preparation, the input states are  $|\psi_a\rangle$  and  $|\psi_b\rangle$ . After the twin photon passes through the two beam splitters (BS)  $BS_1$ ,  $BS_2$  and a phase

shift, the twin photon state has the form (without normalization)

$$|\psi_a\rangle(e^{i\varphi}|u_1\rangle-|d_1\rangle)|\psi_b\rangle(|u_2\rangle+|d_2\rangle). \quad (2)$$

Here  $u_i$  and  $d_i$  ( $i = 1, 2, 3, 4$ ) represent the two path of the photon pass  $\text{BS}_i$ , which is shown in Fig. 2. When they reach  $\text{BS}_3$ ,  $\text{BS}_4$ , we can obtain

$$|\psi_a\rangle\left[e^{i\varphi}(|u_3\rangle+|d_3\rangle)-(|u_4\rangle+|d_4\rangle)\right]|\psi_b\rangle\left[(|u_3\rangle-|d_3\rangle)+(|u_4\rangle-|d_4\rangle)\right]. \quad (3)$$

Only considering the terms containing  $u_3$  and  $d_4$ , we can obtain

$$-e^{i\varphi}|\psi_a\rangle|u_3\rangle|\psi_b\rangle|d_4\rangle-|\psi_a\rangle|d_4\rangle|\psi_b\rangle|u_3\rangle.$$

Then after coincidence in the sequence of  $u_3$  and  $d_4$ , the final state is

$$|\psi'\rangle=-e^{i\varphi}|\psi_a\rangle|\psi_b\rangle-|\psi_b\rangle|\psi_a\rangle. \quad (4)$$

In this way, we realize the controll-SWAP gate with the control on the path of the twin photon and SWAP on the polarization of it. Since we do not choose any basis for measurement, the coincidence rate of the two detectors is proportional to

$$\text{Tr}|\psi'\rangle\langle\psi'|\propto 1+|\langle\psi_a|\psi_b\rangle|^2\cos\varphi. \quad (5)$$

In this way, we derive the visibility of the interferometer

$$v=|\langle\psi_a|\psi_b\rangle|^2=\text{Tr}\rho_a\rho_b. \quad (6)$$

We obtain this result based on two pure states  $|\psi_a\rangle$  and  $|\psi_b\rangle$ , however, it can also be demonstrated that for input of single-qubit mixed states  $\rho_a$  and  $\rho_b$ , we still have the relation  $v=\text{Tr}\rho_a\rho_b$ .

There are many possible ways of utilizing this result. For general single-qubit states, we can measure the fidelity  $\langle\psi|\rho|\psi\rangle$  of  $\rho$  with a pure state  $|\psi\rangle$ , overlap  $\text{Tr}\rho_a\rho_b$  between  $\rho_a$  and  $\rho_b$ , purity  $\text{Tr}\rho^2$  of a mixed state  $\rho$  and Hilbert-Schmidt distance  $d^2(\rho_a, \rho_b) = 1/2\text{Tr}(\rho_a - \rho_b)^2$  between  $\rho_a$  and  $\rho_b$  [2, 3].

Our experimental set-up is shown in Fig. 2(b). In the experiment, for simplicity, we adjust HWP and tiltable QWP in the pump path to choose the real numbers  $a$  and  $b$  in state (1). We use HWP and quartz in the signal (idle) path to prepare input states. Two

lenses ( $f = 300\text{ mm}$ ) are properly placed to increase the detection efficiency of the single-mode fiber [9]. We add four QWPs in the set-up to compensate the phase shift between horizontal and vertical polarization due to reflection. We use a piezoelectric ceramics (PZT) in reflective mirror  $M_1$  as a phase shift. In the experiment, we first find the two HOM interferometers dip using the coincidence of  $D_1$  and  $D_4$ ,  $D_2$  and  $D_3$ . Then we use the coincidence of  $D_2$  and  $D_4$  to observe the interference curve as we adjust the voltage of PZT.

First, we input states into the network with the form  $\rho_a \otimes \rho_b$ . In Fig. 3(a), We choose  $\rho_a = |H\rangle\langle H|$  and  $\rho_b = (\cos 2\theta|H\rangle + \sin 2\theta|V\rangle)(\cos 2\theta\langle H| + \sin 2\theta\langle V|)$  ( $\theta$  is the angle between the optical axis of the HWP and the vertical axis). In Fig. 3(b), we choose a pure state  $\rho_a = (\cos 2\theta|H\rangle + \sin 2\theta|V\rangle)(\cos 2\theta\langle H| + \sin 2\theta\langle V|)$  and a mixed state  $\rho_b = \begin{pmatrix} 0.5 & 0.29 \\ 0.29 & 0.5 \end{pmatrix}$  which is prepared through a HWP ( $\theta = 22.5^\circ$ ) and a  $6.5\text{ mm}$  quartz. From the figures, we can see that experimental dots are in agreement with the theoretical curves. A similar experiment for measurement of the overlap of two single qubit states can be seen in Ref. [10].

For a general two-qubit state  $\rho_{ab}$ , we can obtain the relation

$$v = \text{Tr}\rho_{ab}W = \text{Tr}\rho_{ab}^{T_a}|\Phi^+\rangle\langle\Phi^+| = \langle\Phi^+|\rho_{ab}^{T_a}|\Phi^+\rangle, \quad (7)$$

where  $W$  is the SWAP operator in the form  $|\Phi^+\rangle\langle\Phi^+|^{T_a}$  ( $|\Phi^+\rangle = 1/\sqrt{2}(|HH\rangle + |VV\rangle)$ ) and  $T_a$  represents partially transposition about the system A. This result agrees well with the Ref. [3]. Then according to Peres-Horodecki criterion [11], if  $v < 0$ , we can make sure that the state  $\rho_{ab}$  is entangled. Hence the operator  $W$  is just the entanglement witness operator for these states. However, if  $v > 0$ , we can't determine whether  $\rho_{ab}$  is entangled or not. In this way, we associate entanglement-witness measurement with the sign of  $v$ . In addition, since local unitary transformations cannot alter the entanglement of one state, for all pure states and some kinds of mixed states, we can quantitatively measure the entanglement of them with some proper local unitary transformations. Moreover, for some special states, such as, the two-qubit Werner state and the nonmaximally entangled state  $a|HV\rangle \pm b|VH\rangle$ , the absolute values of  $v$  are just equal to their concurrence [12]. In this sense, this scheme can be used for quantitative entanglement-witness. So the set-up becomes an “entanglementmeter” for some partially known states and may have important uses especially when the resources are scarce.

In the following, we input entangled states into the network. In Fig. 3(c), we select the input states as  $\cos 2\theta|HH\rangle \pm \sin 2\theta|VV\rangle$ , we find the visibility does not change with the value

of  $\theta$  as expected. However, In Fig. 3(d), the input states become  $\cos 2\theta|HV\rangle \pm \sin 2\theta|VH\rangle$ , we can get a sinusoidal curve which is in accordance with the value of concurrence after experimental correction [13].

Fig. 4 shows the entanglement-witness measurement. In order to demonstrate the inverse of the interference curve of entangled state compared with the one of the disentangled state, in principle, we need to scan the whole interference curves of the two cases. But due to the phase instability caused by light path and PZT, we can not obtain a perfect interference curve. So we first adjust the voltage of PZT and let the interference of the entanglement stabilize at some place, such as the maximum or minimum. Next we replace the entangled state with a disentangled one ( $|H\rangle \otimes |H\rangle$ ) to observe its interference. In order to ensure the phase stability during the whole process, finally we return to the original entangled state. For each input state, we consecutively note down 50 dots. For the three input states in each figure, totally we can obtain 150 dots. In Fig. 4(a) and (b), we input the entangled state  $\frac{1}{\sqrt{2}}(|HV\rangle - |VH\rangle)$  and we can see the obvious flip of the coincidence when replacing the input states; while for Fig. 4(c) and (d), the input state is  $\frac{1}{\sqrt{2}}(|HV\rangle + |VH\rangle)$ , there are no obvious changes when input states is alternated. Here we demonstrate entanglement-witness measurement of the single state. For the other Bell states, we only need unilateral local unitary transformations. We can generalize our set-up to other entangled states such as, the Werner states. It just needs to prepare and input the states before the Hong-Ou-Mandel interferometers.

As we know, for the general entanglement-witness measurement, first the witness operators are decomposed into a pseudomixture of local operators, then by adding the resulting expectation values of local operators with the corresponding positive or negative weight, the value of witness operator is obtained [14]. There also exists “structural” physical approximations (SPA) for estimating the minimum eigenvalue of a transformed density matrix to detect quantum entanglement according to positive maps separability criterion [1, 15] (also see [16]). Compared with the method above and Ref [3], we find a method for direct detection of witness operators utilizing our scheme and physically implement the positive but not completely positive map, transposition, from another point of view.

In conclusion, we put forward a scheme to simulate the quantum network shown in Fig. 1 using linear optical elements, which is based on two Hong-Ou-Mandel interferometers. As a basic building block, our scheme can be cascaded to apply to high dimensional systems[17].

It can be used to estimate functionals of high dimensional density matrices and avoid the necessity of a complete state reconstruction. For example, it can evaluate the spectrum, the extremal eigenvalues and eigenvectors of density matrices. Based on this, the network may have potential applications in estimating some properties of quantum channels, because a quantum channel is a trace preserving linear map, which maps density operators into density operators [2]. Recently, H. A. Carteret give a method that can determine the spectrum of a partially transposed density matrix using the similar network without the addition of noise to make the spectrum non-negative [18].

Experimentally, we realize the scheme using linear optical elements. We perform the measurement of overlap of two pure states and that of one pure state and one mixed state. The results agree well with the theory. Our set-up can be used to measure entanglement for all pure states and some kinds of mixed states and implement entanglement-witness measurement for states with non-positive partial transposition. We associate the value of the interference visibility of the state with its concurrence to measure entanglement and associate the inverse of the interference curve compared with the one of the disentangled state with its entanglement to demonstrate entanglement-witness measurement. We experimentally and directly detect the value of witness operator and observe the obvious flip of the coincidence to show their entanglement. From the other perspective, we physically implement a positive but not completely positive map, transposition. However, usually the map is indirectly implemented through SPA [15]. Using our set-up, we realize the Fredkin (controlled-SWAP) gate, which may be helpful for quantum information processing in the future.

The authors would like to thank Qin Wang, Bi-Heng Liu and Guo-Yong Xiang for helpful discussions. This work was funded by the National Fundamental Research Program (2001CB309300), National Natural Science Foundation of China, Innovation Funds from Chinese Academy of Sciences, and Program for New Century Excellent Talents in University.

---

[1] P. Horodecki and A. Ekert, Phys. Rev. Lett. **89**, 127902 (2002).

[2] A. Ekert, C. M. Alves, D. K. L. Oi, M. Horodecki, P. Horodecki, and L. C. Kwek, Phys. Rev. Lett. **88**, 217901 (2002).

- [3] R. Filip, Phys. Rev. A **65**, 062320 (2002).
- [4] J. Fiurasek *et al.*, Phys. Rev. Lett. **89**, 190401 (2002).
- [5] B. Terhal, Linear Algebr. Appl. **323**, 61 (2001); M. Lewenstein *et al.*, Phys. Rev. A **62**, 052310 (2000); *ibid.* **63**, 044304 (2001); D. Brub *et al.*, J. Mod. Opt. **49**, 1399 (2002).
- [6] C. K. Hong, Z. Y. Ou, and L. Mandel, Phys. Rev. Lett. **59**, 2044 (1987).
- [7] A. G. White *et al.*, Phys. Rev. Lett. **83**, 3103 (1999).
- [8] T.-C. Wei, J. B. Altepeter, D. Branning, P. M. Goldbart, D. F. V. James, E. Jeffrey, P. G. Kwiat, S. Mukhopadhyay, and N. A. Peters, Phys. Rev. A **71**, 032329 (2005).
- [9] Z. W. Wang *et al.*, Phys. Lett. A 344, 346 (2005).
- [10] M. Hendrych *et al.*, Phys. Lett. A 310, 95 (2003).
- [11] A. Peres, Phys. Rev. Lett. **96**, 1413 (1996); M. Horodecki, P. Horodecki, and R. Horodecki, Phys. Lett. A **223**, 1 (1996).
- [12] S. Hill and W. K. Wootters, Phys. Rev. Lett. **78**, 5022 (1997); W. K. Wootters, Phys. Rev. Lett. **80**, 2245 (1998).
- [13] In Fig. 3(c), we derive the horizontal line according to the experimental data, which should be 1 according to theoretical calculation. The main causes of the decrease of visibilities are mismatch of spatial modes and non-perfect phase compensation. In Fig. 3(d), we incorporate the experimental correction based on Fig. 3(c) into the theoretical curve.
- [14] O. Guhne, P. Hyllus, D. Bru, A. Ekert, M. Lewenstein, C. Macchiavello, and A. Sanpera, Phys. Rev. A **66**, 062305 (2002).
- [15] P. Horodecki, Phys. Rev. A **68**, 052101 (2003).
- [16] T. A. Brun, Quantum Inf. Comput. **4**, 401 (2004).
- [17] C. M. Alves, P. Horodecki, D. K. Oi, L. C. Kwek, and A. K. Ekert, Phys. Rev. A **68**, 032306 (2003); Y.-K. Bai, S.-S. Li, and H.-Z. Zheng, Phys. Rev. A **69**, 052305 (2004).
- [18] H. A. Carteret, Phys. Rev. Lett. **94**, 040502 (2005).

**FIG. 1.** The quantum network is proposed by A. K. Ekert *et al.* [Phys. Rev. Lett. 88, 217901 (2002)], which is comprised of two Hadamard gates, phase shift  $\varphi$ , and a Fredkin (controlled-SWAP) gate. The network can be used for direct estimations of linear and nonlinear functionals of state. The probability of finding the control qubit in state  $|0\rangle$  is given by  $v = \text{Tr}\rho_a\rho_b$ .

**FIG. 2.** Fig. 2(a) is our sketch map to implement the network shown in Fig. 1. The spontaneous parametric down-conversion (SPDC) process is used to produce entangled states. The

next process is state preparation, we can generate states, as we require. In the following, we put the prepared states into our interferometer. We use two Hong-Ou-Mandel interferometers and post-selection to realize the controlled-SWAP operation. The path of the two-photon is selected as the control qubit and the target qubits are the polarization of the twin photon. The two detectors are used for post-selection. Fig. 2(b) is our experiment set-up. H and Q represent half and quarter wave plate (QWP) respectively.  $B_i$  ( $i = 1, 2, 3, 4$ ) is 50/50 beam splitter.  $M_1$  and  $M_2$  are two reflective mirrors. We use a piezoelectric ceramics (PZT) in  $M_1$  as a phase shift. Before the detector  $D_i$  ( $i = 1, 2, 3, 4$ ) is interference filter (IF) (bandwidth 4.62 nm). The HWP and QWP in pump path is used to prepare entangled or disentangled states. The 4 four QWPs in the signal (idle) path are used to compensate the phase shift between horizontal and vertical polarization due to reflection.

**FIG. 3.** Interference visibility versus input state. The dots are the experimental data and the curves are based on theoretical calculation. For Fig. 3(a) and (b), the horizontal axis is the angle  $\theta$  between the optical axis of the HWP in signal path and the vertical axis. In Fig. 3(a), we measure the overlap of two pure state  $|H\rangle$  and  $\cos 2\theta|H\rangle + \sin 2\theta|V\rangle$ ; in Fig. 3(b), the figure is the overlap of a variable pure state  $\cos 2\theta|H\rangle + \sin 2\theta|V\rangle$  and a mixed state  $\begin{pmatrix} 0.5 & 0.29 \\ 0.29 & 0.5 \end{pmatrix}$ .

For Fig. 3(c) and (d), the horizontal axis is the angle between the optical axis of the HWP in pump path and the vertical axis.

**FIG. 4.** Figures to demonstrate entanglement-witness measurement. Due to many practical limitations, we can't obtain a perfect interference curve. So we first adjust the voltage and let the interference of the entanglement stabilize at some place, such as at the maximum or minimum. Next we replace the entangled state with a disentangled one to observe its interference. In order to ensure the phase stability during the whole process, finally we return to the original entangled state. For each input state, we consecutively note down 50 dots. For the three input states in each figure, totally we can obtain 150 dots. In Fig. 4(a) and (b), the input state is  $\frac{1}{\sqrt{2}}(|HV\rangle - |VH\rangle)$ , we can see the obvious flip of the coincidence when replacing the input states; while for Fig. 4(c) and (d), the input state is  $\frac{1}{\sqrt{2}}(|HV\rangle + |VH\rangle)$ , we can see no obvious changes when replacing the input states.

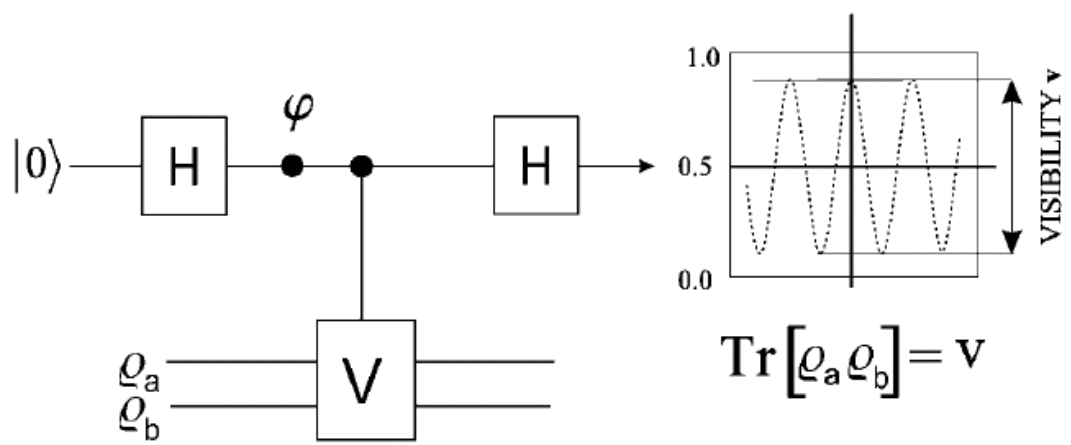


FIG. 1

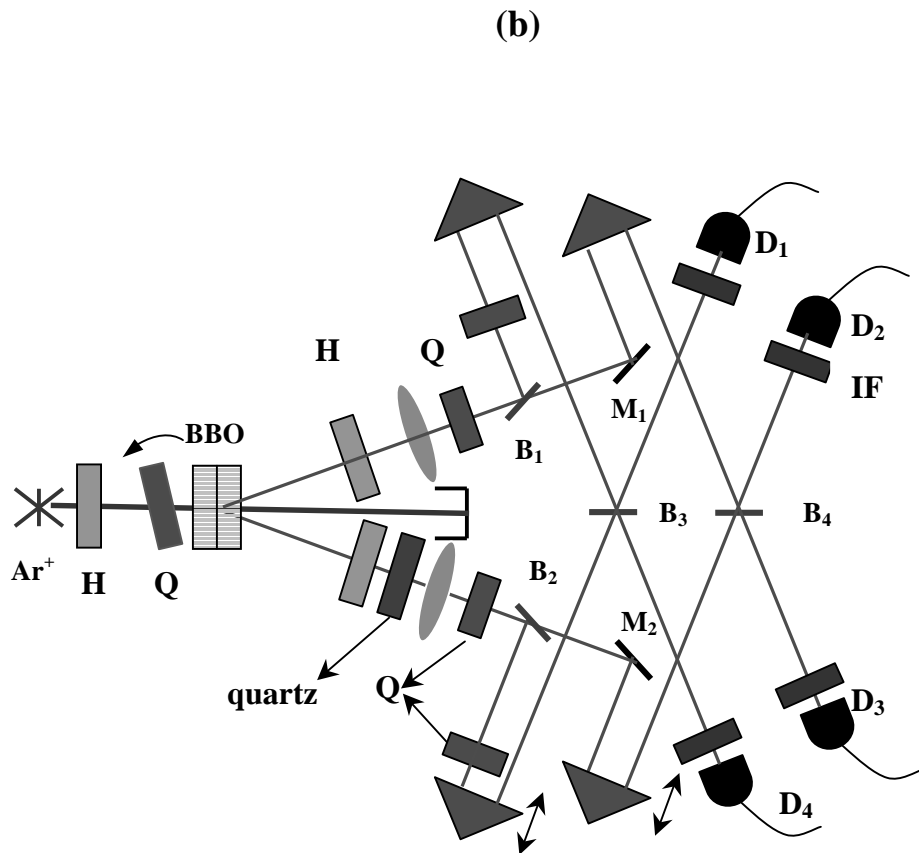
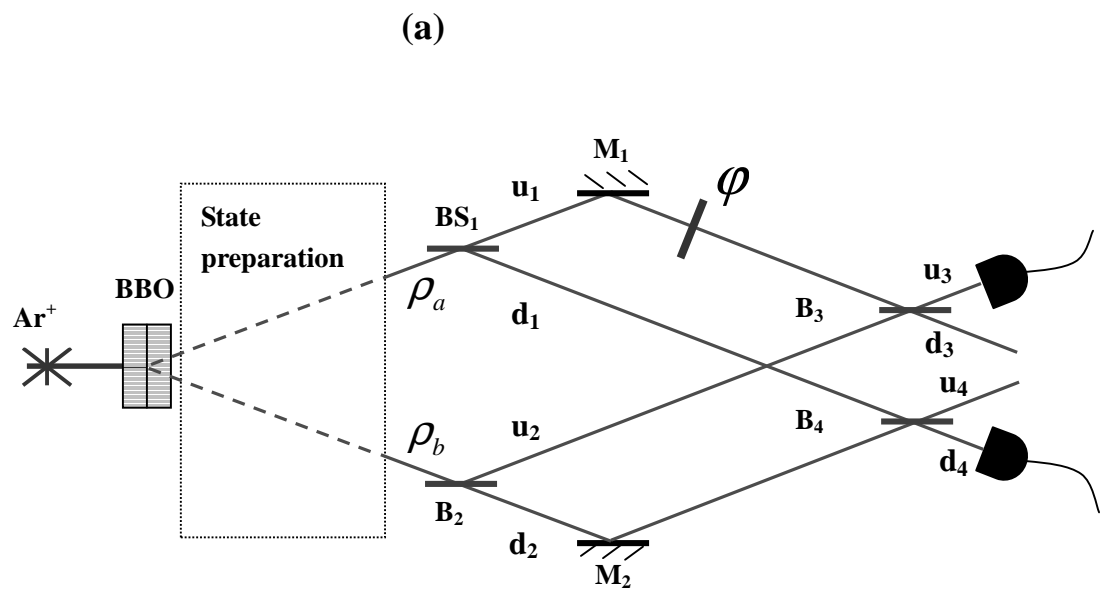
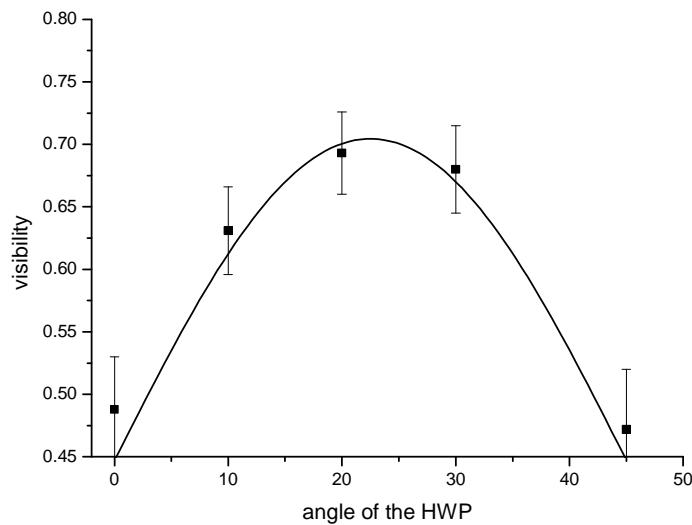


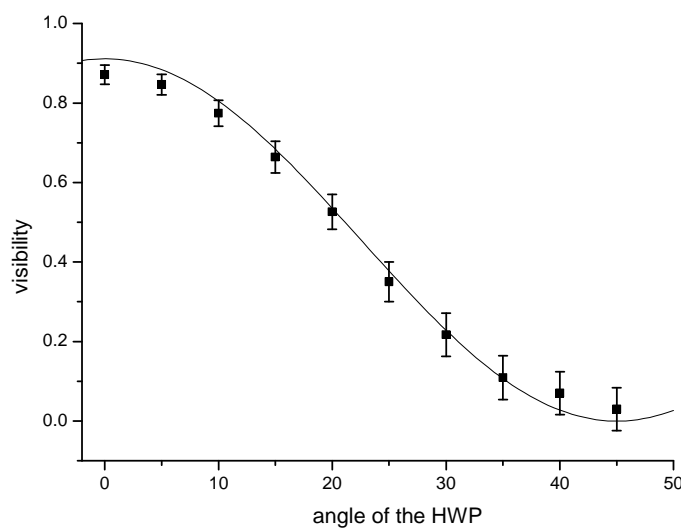
FIG. 2



**(a)**



**(b)**



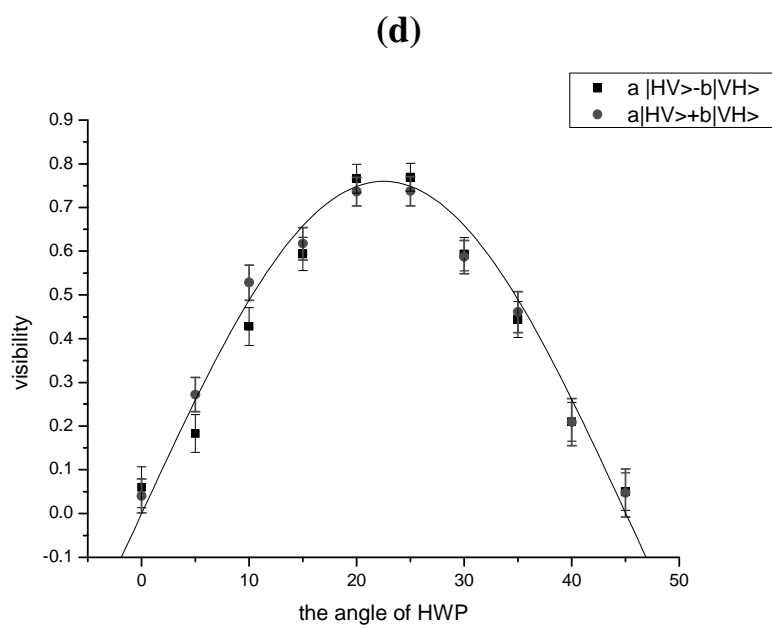
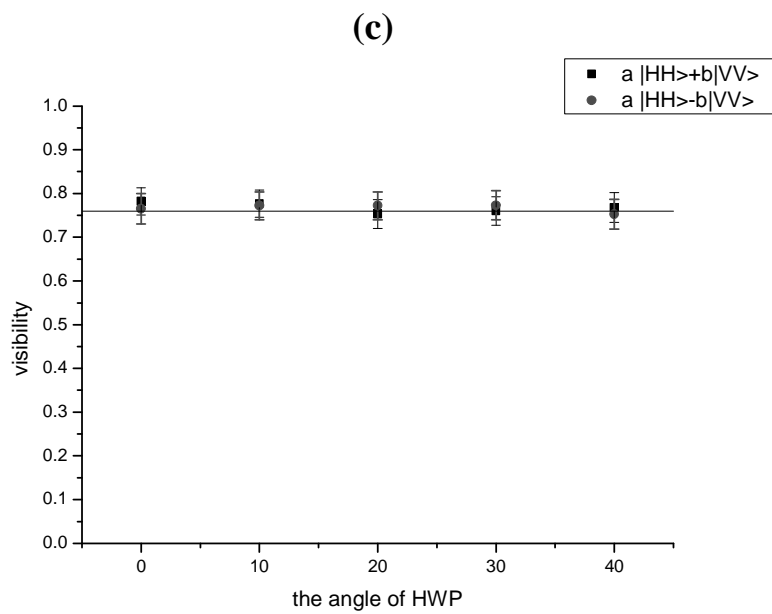
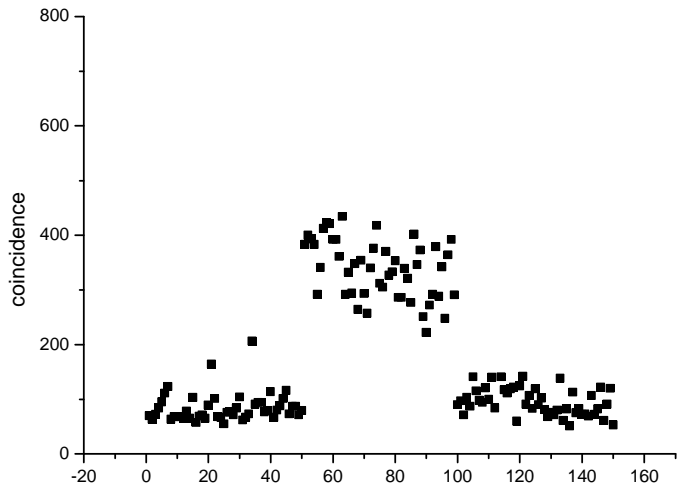
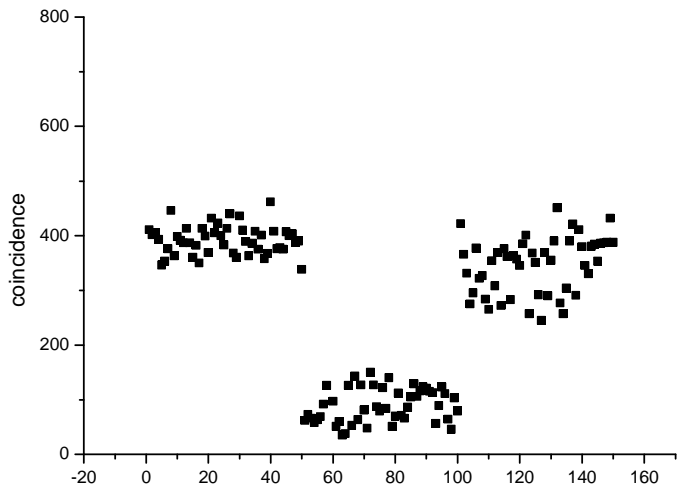


**FIG. 3**

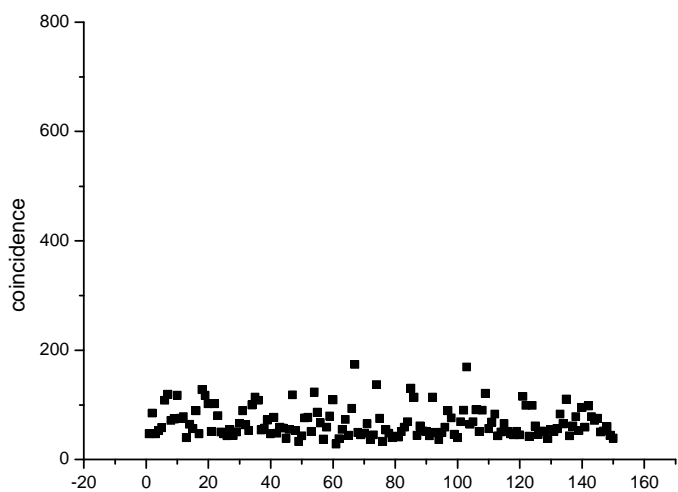
**(a)**



**(b)**



**(c)**



**(d)**

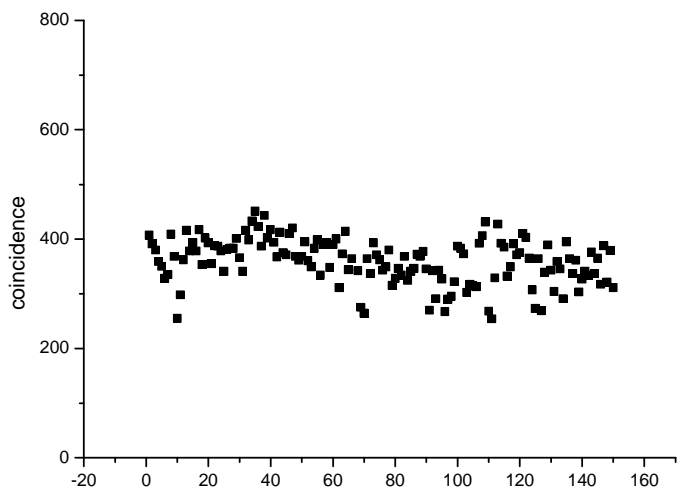


**FIG. 4**